Luo *et al.*
Journal of Engineering and Applied Science (2022) 69:105
https://doi.org/10.1186/s44147-022-00160-x

Journal of Engineering and Applied Science

RESEARCH

Open Access

Characteristics of reducing local scour around cylindrical pier using a horn-shaped collar

Kedian Luo[1*], Yuhang Si[1], Shaohua Lu[1], Boyang Liang[1] and Hongliang Qi[1,2]

*Correspondence: 2019901460@chd.edu.cn

[1] School of Highway, Chang'an University, Xi'an 710064, Shaanxi, China
[2] Key Laboratory for Special Area Highway Engineering of Ministry of Education, Chang'an University, Xi'an 710064, Shaanxi, China

Abstract

Local scour is the major cause of bridge water damage. The sediment in the riverbed around the pier is eroded and transported by water flow, leading to a loss of bridge foundation stability. In this study, a horn-shaped collar was proposed to mitigate local scour around bridge piers. The three design parameters (bottom diameter, vertical height, and curvature shape index) of the horn-shaped collar were studied under clear water condition, and the number of experimental tests was reduced to 25 by using Taguchi's method. Main effect analysis was used to determine the optimum design parameters for the horn-shaped collar. The results show that the three design parameters have a significant effect on the scour reduction capacity of the horn-shaped collar, with the bottom diameter of the collar making the greatest contribution. The optimum values for the bottom diameter, vertical height, and curvature shape index are 5*D*, 0.25*D*, and 4, respectively (*D* represents the diameter of the pier), and the optimized shape of the horn-shaped collar reduces the maximum scour depth around the pier by 100% compared to the unprotected case. Based on the experimental data, prediction equations are developed for the maximum scour depth protected by a horn-shaped collar.

Keywords: Bridge engineering, Clear water, Local scour, Optimal design, Taguchi's method, Three-dimensional collar

Introduction

Local scour is a phenomenon resulting from water interacting with bridge piers. When the water is blocked by structures, such as bridge piers and abutments, rapid changes of the water around the piers occur, which causes the formation of three-dimensional vortices. Shear stress on the sediment surface near the bridge piers is generated by different vortices, which vigorously washes away and transports the upstream sediment in front of the bridge piers. Finally, scour hole appears around the bridge pier. Local scour is one of the primary contributors to bridge damage [1]. A study conducted by the FHWA in 1973 on 383 bridge failures caused by catastrophic floods found that 25% involved damage to piers and 72% involved damage to abutments [2]. Among the 106 bridge collapse accidents in China from 2000 to 2014, 78% were caused by floods [3]. Therefore, the study on local scour protection measures for bridge piers has become a significant topic all over the world.

In recent years, many domestic and foreign researchers have carried out a lot of research on the countermeasures to local scour around bridge piers. These countermeasures can be classified into two categories, i.e., (a) active countermeasures and (b) passive countermeasures [4]. The countermeasure adopted to weaken the scouring force of the water through compromising the strength and deflecting the direction of the incoming water is called active countermeasure. Typical methods of active countermeasures include collar [5], sacrificial piles [6], ring-wing piers [7], and pier slots [8]. A passive countermeasure improves the resistance of sediment to local scour. Traditional methods of passive countermeasures consist of expanding foundation protection, riprap protection [9], and partial riprap grouting. Among the active countermeasures, the collar plays a role in reducing local scour by weakening the downflow in front of the bridge pier [10]. Compared with other scour reduction measures, collars have been widely used due to their advantages of simple construction and low maintenance costs [11].

Kumar et al. [12] studied the influence of the size and installation height of the collar on the local scour. Through data processing and analysis, a formula for the maximum scour depth prediction around a circular pier equipped with a collar was obtained. Wang et al. [13] investigated the influence of the external diameter, installation height, and protection range of the collar on the development and features of scour hole around the pier and observed the distribution of the time-dependent scour depth around the pier. In conclusion, as the external diameter of the collar increases, the maximum scour depth decreases, and the protective effect of the collar grows; the increase of installation height results in the reduction of the scour resistance of the collar. When collar is installed beyond a height of 25% of the water depth, the collar provides slight protection [14].

To obtain a better protective effect, researchers designed and studied collars with different shapes. The novel collar consists of two main design concepts: one is changing the shape of the flat collar, and the other is a three-dimensional collar design. For the modified flat collar, Jahangirzadeh et al. [15] studied the influence of rectangular and circular collars on the scour depth around the bridge pier through laboratory model experiments and numerical methods. Compared with a circular collar, a rectangular collar has better protection to the sediment surface; it reduces maximum scour depth around piers by 79%. Raeisi and Ghomeshi [16] proposed an elliptical collar to weaken the downstream vortex through interference on the water flow downstream of the bridge pier, which has better performance than the ordinary circular collar. For the three-dimensional collar, Bestawy et al. [17] developed a conical collar, which was found to have a good effect on reducing scour around the pier through a single pier model experiment, and the scour depth downstream side of the pier was reduced by 61.1%. Chen et al. [18] proposed a new type of collar with a hook. Laboratory and numerical tests showed that the maximum downflow is greatly mitigated, and the intensity of the horseshoe vortex is correspondingly reduced accordingly. Based on the existing flat collar, Valela et al. [11] proposed a three-dimensional collar, which can guide the horseshoe vortex into the cavity of the collar and resist the scour caused by accelerated water flow on both sides of the bridge pier. A numerical model was applied in the iterative design of the collar profile. Subsequent model experiments were carried out to verify the scour resistance of the optimized three-dimensional collar. The results demonstrated that the reduction rate of maximum scour depth and scour volume of the improved collar is 46.6% and 30.8%, respectively [19]. These research results above prove that the shape of the collar has a significant effect on the reduction of local scour around the pier.

There are many types of studies on the scour reduction effect of the flat collar, while the study on the scour reduction effect of the three-dimensional collar is still in the exploratory stage, especially the research on the size and shape of the three-dimensional collar. Therefore, this study proposes a horn-shaped collar, and the influence of its bottom diameter, vertical height, and curvature shape index on scour reduction effect is studied through model tests. Optimal design parameters of the horn-shaped collar and the relationship between collar shape and scour depth are obtained.

Methods

Collar geometry parameters

The anti-scour ability of the collar is mainly determined by the properties of water flow, the properties of sediment in the river bed, the installation height of the collar, and its geometric shape [20], especially the geometric shape of the collar, which is the main factor affecting its scour reduction effect. Compared with the flat collar, the shape characteristics of the horn-shaped collar are controlled by its bottom width (W), vertical height (h), curvature shape equation $f(x)$, and other factors, as shown in Fig. 1a. In terms of the curvature shape equation $f(x)$ of the collar, referring to [11], a cubic polynomial was used to control the linear shape of the cross section of the three-dimensional collar. In order to simplify the expression of collar curvature, the low-order term was omitted, and function $f(x) = kx$ was selected, where k is the coefficient and n is the curvature shape index. When the bottom diameter of the collar, the vertical height, and the curvature shape index n is determined, the coefficient k can be calculated by the curvature shape function of the collar, thereby the shape of the collar is obtained. The three-dimensional structure is shown in Fig. 1b. A 3-D printer was used to produce the horn-shaped collar with different shapes.

Experimental setup

The experiments were carried out in the key laboratory for special area highway engineering of Ministry of Education at Chang'an University. As shown in Fig. 2, the test

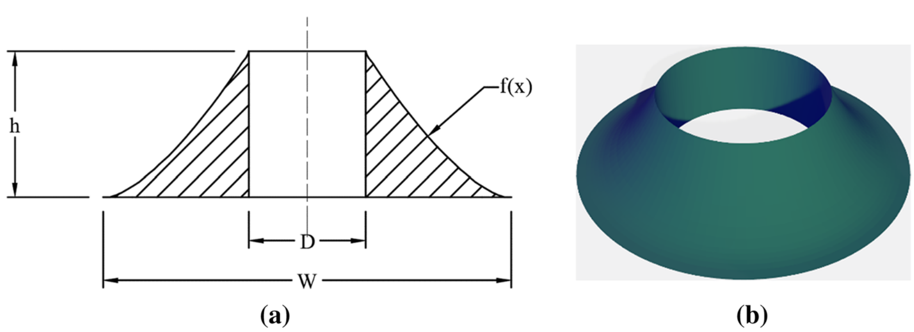

Fig. 1 Schematic diagram of horn-shaped collar. **a** The cross-section view and shape parameters of the horn-shaped collar (D is the pier diameter). **b** Three-dimensional model of the horn-shaped collar

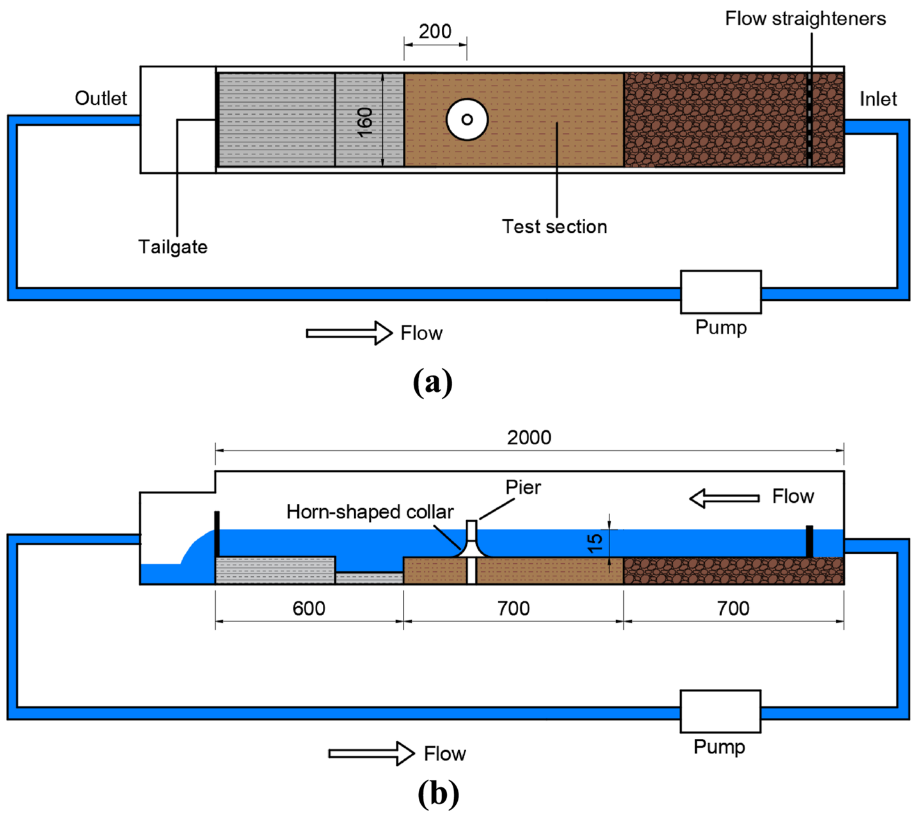

Fig. 2 Schematic diagram of the test flume (unit: cm). **a** Top view. **b** Cross-section view

system consists of a water pump, a sharp edged weir, a test flume, a sedimentation tank, and a tailgate.

The test flume is 20.0 m long, 1.6 m wide, and 0.7 m high. The side walls and bottom of the flume are plastered with cement mortar. The test flume is divided into three parts: the steady flow section, the test section, and the outlet section. The length of the steady flow section is 7.0 m, and the flow straighteners are set at the entrance to make the water flow smoothly and evenly. The test section is 7.0 m long, and 0.15-m-thick uniform sand is laid. The median particle size d_{50} of the sand is 1.19 mm, the average particle size d is 1.13 mm, the uniformity coefficient C_u is 14.17, and the curvature coefficient C_c is 1.54. The sand has good and continuous gradation and meets the test requirements. The gradation curve of sand is shown in Fig. 3. A sedimentation tank with a length of 2.0 m, a width of 1.6 m, and a depth of 0.15 m is arranged downstream of the test section. The water depth is constant at 0.15 m above the sediment surface.

The threshold velocity of sediment was calculated by Zhang Ruijin's formula [21]:

$$V_0 = \left(\frac{h}{d}\right)^{0.14}\left(29d + 0.000000605\frac{10 + h}{d^{0.72}}\right)^{0.5} \tag{1}$$

where V_0 is the threshold velocity of the sediment, h is the water depth of the flow, and d is the average particle size of the sediment. All units are in international standard units. For this study, the threshold velocity of the sediment was 0.363 m/s. The test

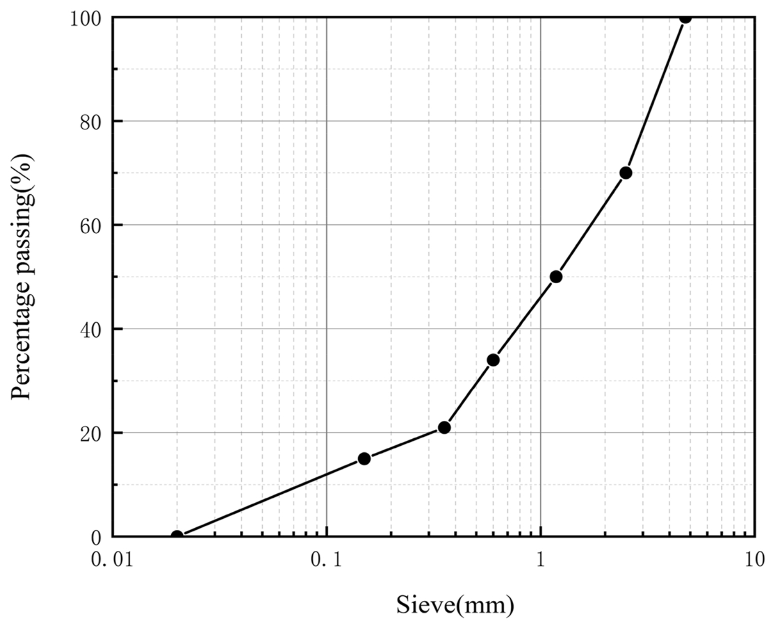

Fig. 3 Gradation curve of the sand

Table 1 Factors and levels in the experiment

Level	Factor		
	W/D	*h/D*	*n*
1	1.5	0.25	1
2	2	0.5	1.5
3	2.5	0.75	2
4	3.5	1.25	3
5	5	1.85	4

condition of this study was clear water scouring, so 95% of the V_0 was taken as the test flow velocity, which was 0.345 m/s.

In order to eliminate the influence of the boundary conditions on the experimental results, the maximum diameter of the pier should be less than 1/10 of the fluid width [22]. A pier with a diameter of 8.0 cm was used in experiments, and the ratio of pier diameter to flow width was 1/20. The bridge pier was arranged on the longitudinal central axis of the test section, 2 m away from the entrance of the outlet section, to ensure that the water flow develops completely before reaching the pier, and the pier bottom was installed at the bottom of the experimental flume. The collar was installed on the surface of the sediment to achieve the best protection effect [23].

Taguchi's design of experiments

According to the purpose of this study, the dimensionless bottom diameter *W/D*, the dimensionless vertical height *h/D*, and the curvature shape index *n* were selected as the primary influencing factors of the horn-shaped collar. Five levels of each influencing factor were selected, as shown in Table 1.

The experiments were designed based on the method with the Orthogonal array L_{25} *(*3^5*)*; the experiments can be reduced to 25 cases. In order to compare and analyze the effect of using the horn-shaped collar to prevent sediment around the pier from local scour, a control test without collar was also set. The design of the horn-shaped collar in each experimental test is shown in Table 2.

Experimental procedure and data measurement

Experimental procedure

1) A pier model and collar were installed according to the plan, and the surface of the sediment was precisely leveled. The elevation of the sediment surface was measured with a laser rangefinder, and the error of the elevation around the pier should be kept within ±1 mm. The elevation of the sediment surface was recorded and used as the datum.
2) The tailgate was closed and the water valve was opened, so that the water surface reached the design depth gradually.
3) The tailgate was opened to make the inlet level of water stable at the design value.

Table 2 Experimental design based on Taguchi's method

No.	**Factors**		
	W/D	***h/D***	***n***
1	1	1	1
2	1	2	2
3	1	3	3
4	1	4	4
5	1	5	5
6	2	1	2
7	2	2	3
8	2	3	4
9	2	4	5
10	2	5	1
11	3	1	3
12	3	2	4
13	3	3	5
14	3	4	1
15	3	5	2
16	4	1	4
17	4	2	5
18	4	3	1
19	4	4	2
20	4	5	3
21	5	1	5
22	5	2	1
23	5	3	2
24	5	4	3
25	5	5	4
26	Without collar		

4) After the scour around the pier reached an equilibrium condition, the water inlet valve and the tailgate were closed to make the water level drop slowly to reduce the impact of drainage on the test results.
5) After the water in the test section was drained, the collar was removed and a laser rangefinder was applied to measure the elevation of the sediment surface.

Data measurement

To observe the change of the scour depth around the bridge pier over time, 12 measuring points were arranged on the pier uniformly by the interval of 30°, and the center point at the pier on the upstream side was 0°. A scale bar was pasted on each measuring point, and the value of the scour depth was recorded by an underwater camera. Timing started when the water flow reached the front of the pier. Due to the rapid development of the scour depth in the initial stage, the observation interval was 1 min in the first 5 min. When the change of the scour depth was small, the interval of observation time can be increased to 5–10 min. If the difference between the two observation values of each measuring point did not exceed 1 mm and lasted for more than 10 min, it was considered that the local scouring has been completed, and the observation can be stopped.

The arrangement of the experimental area before scouring is shown in Fig. 4. According to the extent of the scour hole, size of the measurement area in the experimental tests was 70.0 cm × 90.0 cm. For the control test without collar, it was 50.0 cm × 60.0 cm. The grid of the measuring point on sediment was a square with a side length of 1 cm, and the scour contours were drawn after expanding the measuring point data using the interpolation algorithm.

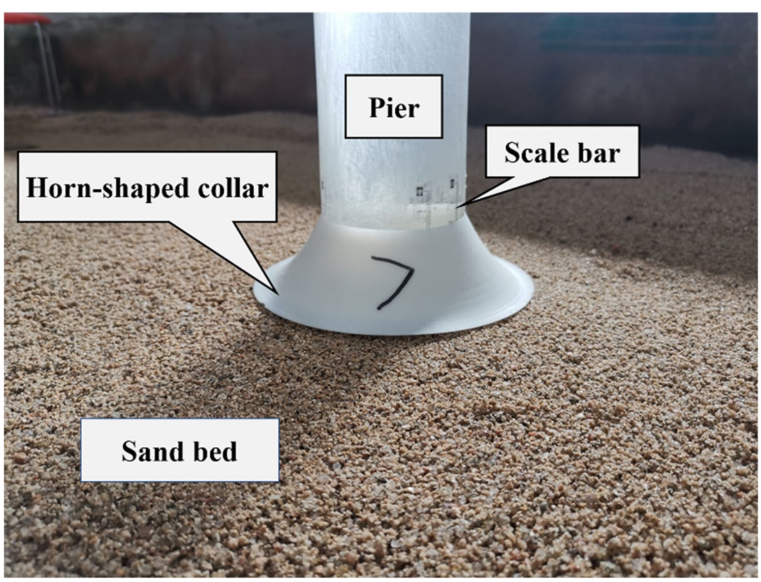

Fig. 4 Configuration of the experimental area before scouring

Results and discussion

Pier without collar

Figure 5a shows the relationship between the local scour depth of the bridge pier and the time when there is no collar protection. The scour depth in front of the pier increased rapidly at the beginning of the experiment, especially in the first 10 min. After that, the change of the scour depth gradually decreased and became stable until the scour equilibrium condition, which was consistent with the development process of the scour hole described above. Figure 5b shows the features of the local scour topography around the pier when there is no collar protection, which is consistent with the abovementioned characteristics of the scour hole around the pier. The development process of the local scour depth around the pier and the characteristics of the local scour hole are similar to the phenomenon described in recent research [5], indicating that the results of this study are correct and credible.

In this study, 40 min after the start of scouring, the difference between two adjacent observations at each measuring point was not more than 1 mm, and the corresponding maximum local scouring depth was 72.0 mm. Sheppard et al. [24] found that the local scour depth and scour time satisfy the following relationship:

$$d_s(t) = a\left[1 - \frac{1}{(1+abt)}\right] + c\left[1 - \frac{1}{(1+cdt)}\right] \tag{2}$$

where *ds(t)* is the maximum scour depth at time *t* and *a*, *b*, *c*, and *d* are all coefficients, which can be determined by the least square method, as shown in Table 3. When the scour time *t* is infinite, the equilibrium scour depth around the pier can be obtained. In this study, the corresponding equilibrium scour depth was 75 mm. According to the theory of Zhao et al. [25], when the scour depth reaches 95% of the equilibrium scour depth, it can be approximately considered that the scour has reached equilibrium, and the corresponding time can be used as the experiment duration. In this study, the time for the scour depth to reach 95% of the equilibrium scour depth was approximately 34 min. To ensure the equilibrium scour depth was reached, the duration of the experiments in this study was 40 min.

Influence of collar on local scour depth and characteristics

Figure 6 illustrates the appearance of scour hole with a horn-shaped collar of case 7. The ability of a horn-shaped collar to reduce local scour depth is closely related to the three parameters studied in this study. In order to quantitatively analyze and compare the scour reduction effect of the horn-shaped collar, this study introduced the percent of the reduction in the scour depth *R* (%), which is expressed as follows:

$$R = (d_{\mathrm{se}} - d_{sec}) \times 100/d_{se} \tag{3}$$

where d_{se} is the maximum scour depth around the pier without collar protection and d_{sec} is the maximum scour depth around the pier with a horn-shaped collar. To ensure the scour time was the same for the control test and the experimental tests, d_{se} adopted the scour depth around the pier at 40 min. The design parameters of each group of test collars and the corresponding *R* (%) are shown in Table 4.

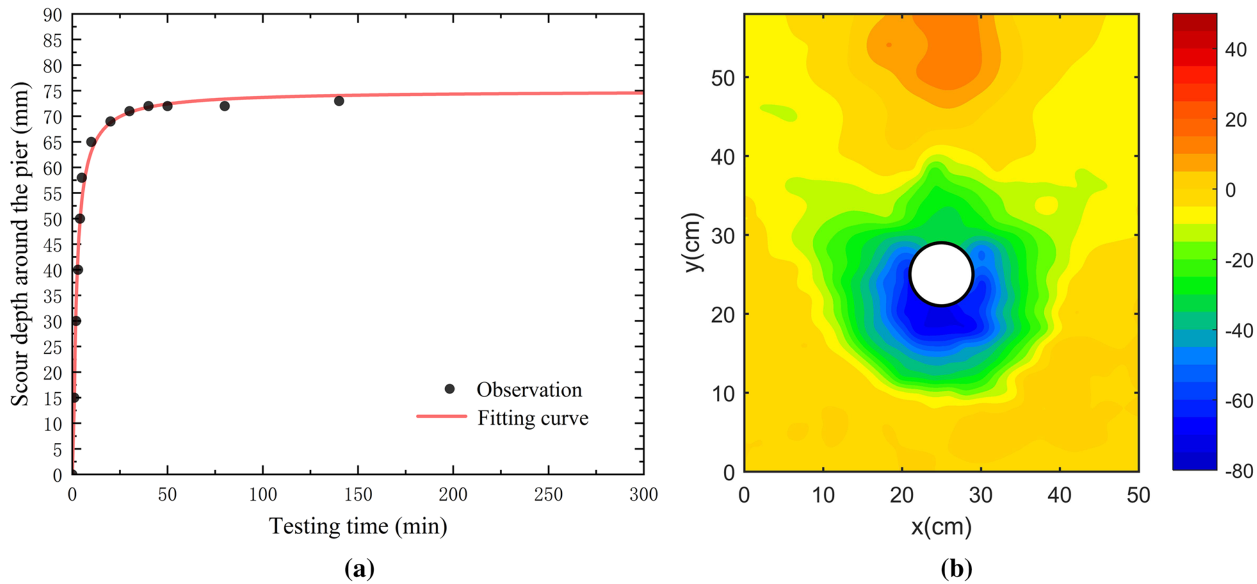

Fig. 5 Characteristics of scour in control test. **a** Time-dependent scour depth without collar protection. **b** Scouring contours of the pier without collar

Table 3 Fitting results

a	b	c	d	R^2
−40.01	10240	115	0.00754	0.9932

Fig. 6 Scour hole appearance of case 7

Table 4 Test results and calculated values of R (%)

Level	Factor			k	Maximum scour depth around the pier (mm)	R (%)
	W/D	h/D	n			
1	1.5	0.25	1	1	70	2.78
2	1.5	0.5	1.5	1.4	61	15.28
3	1.5	0.75	2	1.5	57	20.83
4	1.5	1.25	3	1.25	57	20.83
5	1.5	1.85	4	0.93	68	5.56
6	2	0.25	1.5	0.25	56	22.22
7	2	0.5	2	0.25	58	19.44
8	2	0.75	3	0.094	52	27.78
9	2	1.25	4	0.039	52	27.78
10	2	1.85	1	3.7	76	−5.56
11	2.5	0.25	2	0.056	18	75.00
12	2.5	0.5	3	0.019	32	55.56
13	2.5	0.75	4	0.0046	38	47.22
14	2.5	1.25	1	1.7	69	4.17
15	2.5	1.85	1.5	1.0	61	15.28
16	3.5	0.25	3	0.0020	4	94.44
17	3.5	0.5	4	0.00040	9	87.50
18	3.5	0.75	1	0.60	32	54.17
19	3.5	1.25	1.5	0.32	33	55.56
20	3.5	1.85	2	0.15	45	37.50
21	5	0.25	4	0.00003	0	100.00
22	5	0.5	1	0.25	0	100.00
23	5	0.75	1.5	0.094	0	100.00
24	5	1.25	2	0.039	3	95.83
25	5	1.85	3	0.0036	24	66.67
26	Without collar			-	72	-

Figure 7 shows the scour contours of the experimental tests. Compared with the unprotected pier in the control test, local scour depth around the pier was reduced by the application of the horn-shaped collar. When the bottom diameter W was less than 2.0D, the maximum percent of the reduction in scour depth was 27.78%. For the collar with a 1.5D bottom diameter, the maximum R was 20.83%, and the minimum was 2.78%. At this time, the appearance of the scour hole was similar to that when there was no horn-shaped collar protection. In the case of a collar with a bottom diameter of 2.0D, the scour reduction effect of the collar was significant, and the maximum and minimum R (%) of the collar was 27.78% and −5.56%, respectively. Notably, when the vertical height was 1.85D and the curvature shape index was 1, the scour depth

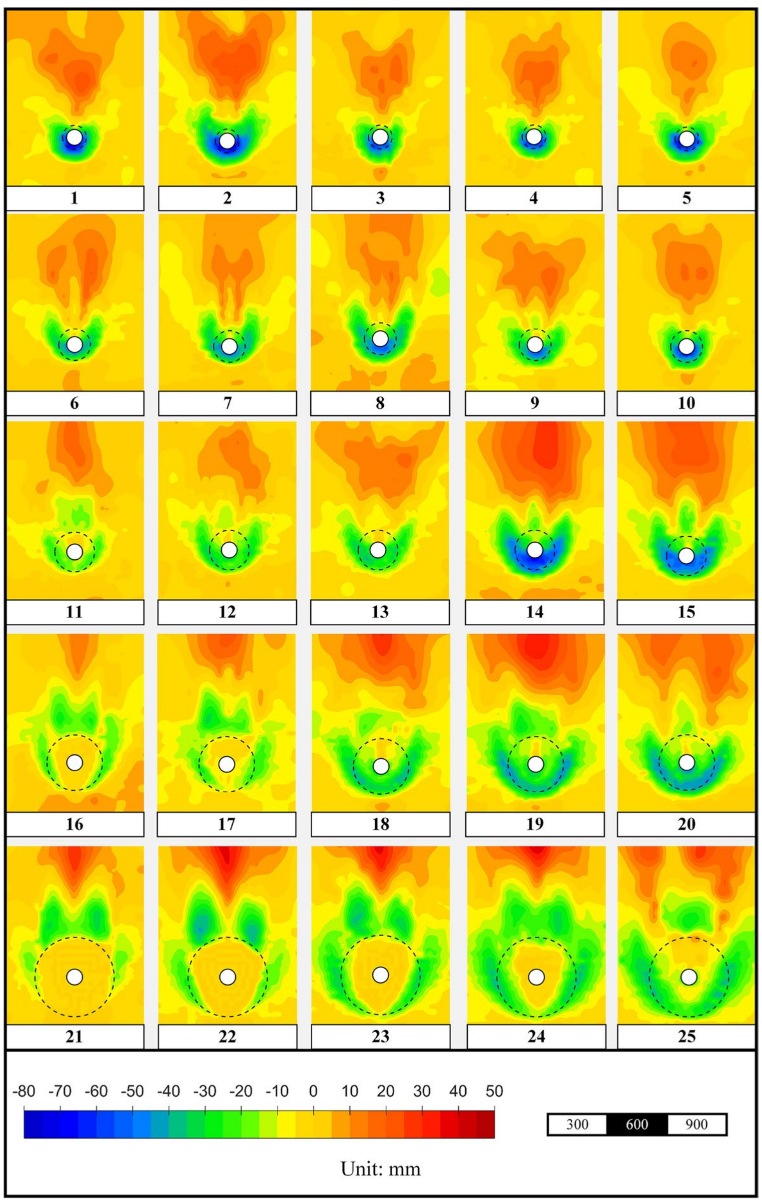

Fig. 7 Scour hole contours of experiment tests

of the collar was 76 mm, which was greater than the scour depth of the control test without a collar. For characteristics of scour holes, deep scour was controlled within the coverage area of the collar, and the shapes of the scour holes were different from that of the control test. The scouring holes extended backward from both sides of the pier, and two obvious uplifted sedimentary ridges appeared on the inside of the scour holes behind the pier. These sedimentary ridges extended from the rear of the collar to the depositional area, dividing the scour hole into three parts. As the vertical height of the collar increased, the two sedimentary ridges became wider gradually.

When the bottom diameter W was 2.5–3.5*D*, the scour reduction ability of the horn-shaped collar was generally improved, and the maximum *R* (%) of the collar reached 94.44%. As the vertical height increased, the ability of the horn-shaped collar to reduce local scour generally decreased, and the horn-shaped collar with a higher curvature shape index had a larger *R* (%). The variation law of scour hole shape was similar to that of the collar with 2.0*D* bottom diameter.

When the bottom diameter of the collar was 5.0*D*, the protective effect of the horn-shaped collar on the pier foundation was the best. At this time, the maximum *R* (%) reached 100%. The depth of the scour hole around the pier was the smallest among experimental tests. The horseshoe vortex only occurred under the edge of the collar, and there was no scour around the pier. The scour and depositional area were far away from the pier.

For the downstream of the pier, as the bottom diameter of the collar increased, the scour depth behind the pier within the horn-shaped collar protection range gradually decreased, and the sediment surface was well protected, but some scour occurred directly behind the collar. After the installation of the horn-shaped collar, a part of the horseshoe vortex moved on the surface of the collar, dropped off at the end of the collar, and generated scour hole on the sediment behind the collar. The scour hole got larger and deeper with the increase of the bottom diameter of the collar. With the reduction of the vertical height, the maximum depth of the scour hole behind the collar moved to both sides.

In conclusion, (1) under the condition that the vertical height h and the curvature shape index n of the collar were constant, the scour reduction effect of the collar increased with the growth of the bottom diameter W; when the bottom diameter W was larger than 3.5*D*, the area of the scour hole on the downstream side of the bridge pier expanded with the vertical height of the collar dropping. (2) When the bottom diameter W of the collar was constant, the scour reduction effect of the collar was affected by the vertical height h and the curvature shape index n. Generally speaking, a collar with a large vertical height and a small curvature shape index had a poor effect on reducing the scour and even aggravated the local scour around the bridge pier.

Main effects analysis of maximum scour depth

For each factor, the average value of the experimental results at the same level is calculated by Eq. (4).

$$T_{ij} = \frac{\sum Y_{ij}}{n}, i = 1, 2, \cdots, m \quad (4)$$

where m is the total number of factors, n is the total number of levels, and Y_{ij} is the experimental result when i^{th} factor at the j^{th} level. Range R_i represents the difference between the maximum and minimum values of T_{ij}, and it can be calculated by Eq. (5).

$$R_i = \max(T_{i1}, \cdots, T_{in}) - \min(T_{i1}, \cdots, T_{in}) \tag{5}$$

R_i reflects the fluctuation of the experimental results of the i^{th} factor at different levels. By sorting the R of each factor, the influence of different factors on the experimental results can be obtained. The larger the value of R, the more significant the effect of this factor on the experimental results. By analyzing the experimental results at different levels of the specified factor, the influence trend of the different levels of the factor on the results can be obtained.

According to the results in Table 5, the bottom diameter of the collar ranked first among three factors. Accordingly, the reduction effect of the maximum scour depth around the bridge pier was strongly influenced by the bottom diameter of the collar. The order of influence of all other factors on the scour reduction effect can be indicated as the vertical height of the collar > curvature shape index.

Figure 8 illustrates the effects of different levels of the same factor on the experimental results. Taking the maximum scour depth around the pier as the evaluation indicator, the smaller the average scour depth, the better the protective effect of the factor at this level on local scour. When the bottom diameter, the vertical height, and the curvature shape index of the horn-shaped collar were $5D$, $0.25D$, and 4, respectively, it can be inferred that the collar has the best protection effect on local scour around the pier. As shown in Table 4, the design parameters of the collar used in the 21st case of experiments are identical with this combination.

Trends in average scour depth of the same factor at different levels revealed that as the bottom diameter of the collar increased, the maximum scour depth around the pier decreased. The increase of vertical height will reduce the protective effect of the horn-shaped collar. And with the growth of the curvature shape index, the scour protection effect of the collar gradually rose. When the curvature shape index of the collar was greater than 2, the variation of the maximum scour depth around the pier caused by the curvature shape index was small. Therefore, considering the construction of the

Table 5 The average value of each level of the factor (mm)

Factor	**Bottom diameter**	**Vertical height**	**Curvature shape index**
Factor level	**Average maximum scour depth**		
1	62.6	29.6	49.6
2	58.8	32	42
3	43.6	36	36.2
4	24.6	42.6	33.8
5	5.4	54.8	33.4
Maximum value	62.6	54.8	49.6
Minimum value	5.4	29.6	33.4
Difference (max-min)	57.2	25.2	16.2
Rank	1	2	3

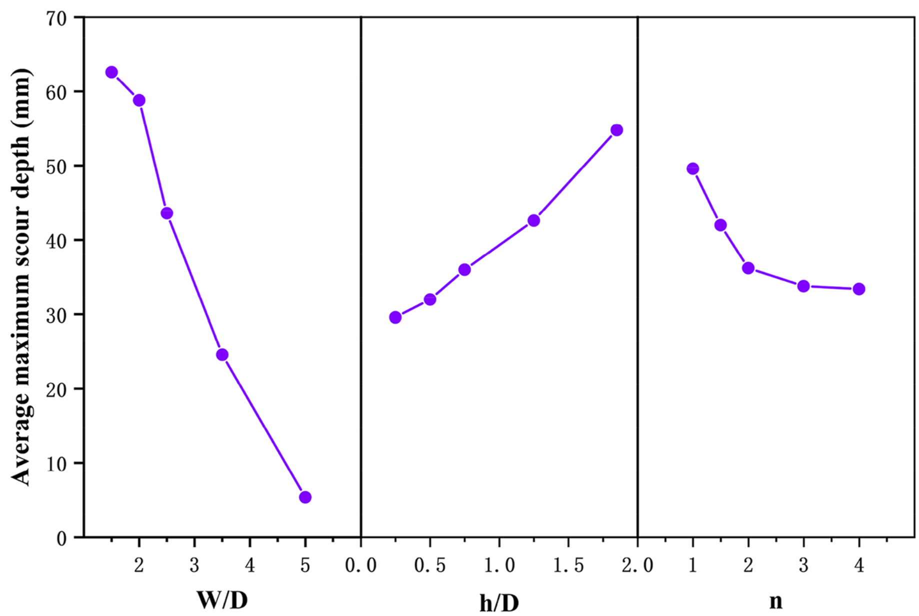

Fig. 8 Main effect plot of the maximum scour depth around the pier

horn-shaped collar, the curvature shape index of the collar can be selected as 2 or 3 to facilitate the construction and save cost while ensuring the protection effect.

Analysis of variance for maximum scour depth

Since the experiment was designed according to a specially developed orthogonal array, it is only a set of full factorial combinations, and confidence analysis is necessary to verify the results of the experiments. ANOVA is a standard statistical technique that can determine the variability of the data to provide a measure of confidence. Therefore, ANOVA was introduced to analyze the experimental results so as to objectively determine whether the factors investigated in the experiment had a significant effect on the experimental results [26].

For ANOVA, the total sum of squared deviations S_T, the sum of squared deviations for individual factors S_A, and the sum of squared deviations of errors S_E should be calculated. The total sum of squared deviations represents the deviation of the experimental data from the mean and can be calculated by the following equation.

$$S_T = \sum_{i=1}^{n} \left(Y_i - \overline{Y}\right)^2 \tag{6}$$

where n is the total number of experiments, Y_i is the result of i^{th} experiment, and $\overline{Y}$ is the average value of Y_i. The sum of squared deviations for individual factors can be calculated by Eq. (7):

$$S_A = \sum_{k=1}^{L} \frac{1}{n_k} \left[\sum_{i=1}^{n_k} (A_{ik} - Y_0)\right]^2 - \frac{T^2}{n} \tag{7}$$

where n_k is the number of experimental tests when the factor level is taken as k, L is the total number of levels, A_{ik} is the value of the experimental result when the factor level is taken as k, Y_0 is the imaginative value of the experiment result, and T is the sum of the deviations of the experimental results from the imaginative value. As the total sum of squared deviations and the sum of squared deviations for each factor are known, the sum of squared deviations of errors can be calculated by the following equation.

$$S_E = S_T - S_A \tag{8}$$

The degree of freedom of the factor is equal to the number of levels of each factor minus one, the total degree of freedom is equal to the total number of experimental cases minus one, and the degree of freedom of error is the difference between the total degree of freedom and the sum of the degree of freedom of each factor. After *DOF* is obtained, the mean square of each factor and error can be obtained by dividing the sum of squared deviations by the degree of freedom.

F-test is applied in the ANOVA to determine the degree of influence of the factors on the results. Since the sum of squared deviations for individual factors and the sum of squared deviations of the errors are independent of each other, the ratio of their mean squares (*MS*) obeys the *F*-distribution, and the *F*-value can be calculated by the following Eq. (9).

$$F_j = \frac{MS_j}{MS_e} \sim F\left(f_j, f_e\right) \tag{9}$$

When $F_j > F_{1-\alpha}(f_j, f_e)$, the factor can be considered to be significant at the significance level α.

The ANOVA results are shown in Table 6. A total of 99%, 95%, and 90% confidence intervals correspond to *F*-values of 5.41, 3.26, and 2.48, respectively. Therefore, it can be concluded that the bottom diameter and vertical height of the horn-shaped collar have a significant effect on reducing the local scour depth around the pier at the 99% confidence interval. At the 90% confidence interval, the three design parameters of the horn-shaped collar had a significant effect on reducing the local scour around the pier. The order of the effect of the factors on the reduction of the maximum scour depth around the pier was bottom diameter > vertical height > curvature shape index, which was consistent with the conclusion of the main effect analysis.

Table 6 Analysis of variance for maximum scour depth

Source	*DOF*	*S*	*MS*	*F*
Bottom diameter of collar	4	11,532.4	2883.1	35.27
Vertical height of collar	4	2044.8	511.2	6.25
Curvature shape index	4	938	234.5	2.87
Error	12	980.8	81.7	1
Sum	24	15,496		

Prediction of the protective effect of horn-shaped collar on local scour

Prediction of R (%)

The percent reductions of scour depth R (%) of the different collars in experimental tests are shown in Fig. 9a. According to the variation of the bottom diameter of the collar W and R (%), the collars can be divided into four groups, $W \leq 2.0D$, $W = 2.5D$, $W = 3.5D$, and $W \geq 5.0D$. When $W \leq 2.0D$, R (%) of different horn-shaped collars was relatively small but close; when $W \geq 5.0D$, R (%) of different horn-shaped collars was relatively large and had similar values, and the R (%) of three types of collars (cases 21 to 23) even reached 100%; when $W = 2.5D$ or $3.5D$, R (%) of each collar is significantly improved compared with $W \leq 2.0D$ but fluctuated more. Figure 9b shows the mean and variance of the average R (%) of the group and the relationship between the average R (%) and the dimensionless bottom diameter (W/D) for each group of tested collars. The R (%) of the four groups of collars was linearly correlated with the collar dimensionless bottom diameter (W/D), and the correlation coefficient reached 0.95. With the increase of W/D, the average R (%) of the collars increased linearly, and this function can be used to predict the average R (%) of a horn-shaped collar with a specific bottom diameter.

Based on the variance of the average R (%) in four groups, it can be concluded that when $W = 2.5D$ or $3.5D$, the scour reduction of each collar was influenced by the vertical height and curvature shape index which mainly controls the cross-section area and the curvature steepness of the horn-shaped collar. For pier protected by a collar with $W = 2.5D$ or $3.5D$, local scour occurred firstly at 30° and 330° in front of the pier, and the curvature steepness of the collar had more influence on the lateral turbulent flow. Therefore, the curvature steepness of the horn-shaped collar δ was chosen as the independent variable and was defined as follows:

$$\delta = A/r^2 \tag{10}$$

where A is 1/2 of the cross-section area of the collar (without area of the pier) and r is the distance between the bottom edge of the collar and the edge of the pier. It can be calculated by $(W-D)/2$. The percent reduction of the scour depth around the pier is a function of the curvature steepness of the horn-shaped collar. A quadratic polynomial fit was used to obtain the function $R(\delta)$, and Eq. 11 shows the fitting result. Figure 10a illustrates the predictive curve.

$$R = 19.76\delta^2 - 80.62\delta + 93.24 \tag{11}$$

Prediction of the maximum scour depth around the pier

The maximum scour depth of the collar is influenced by the shape of the horn-shaped collar. Referring to Fig. 7, the maximum scour depth under the protection of a collar with a flat edge is less than that of a collar with steep edge. Therefore, the curvature steepness can be used to predict the maximum scour depth around the pier. Defining the dimensionless quantity d_{se}/D as the scale of scour depth to avoid the influence of pier geometry on the results, the following relationship can be obtained by observing the scatter plot in Fig. 10b.

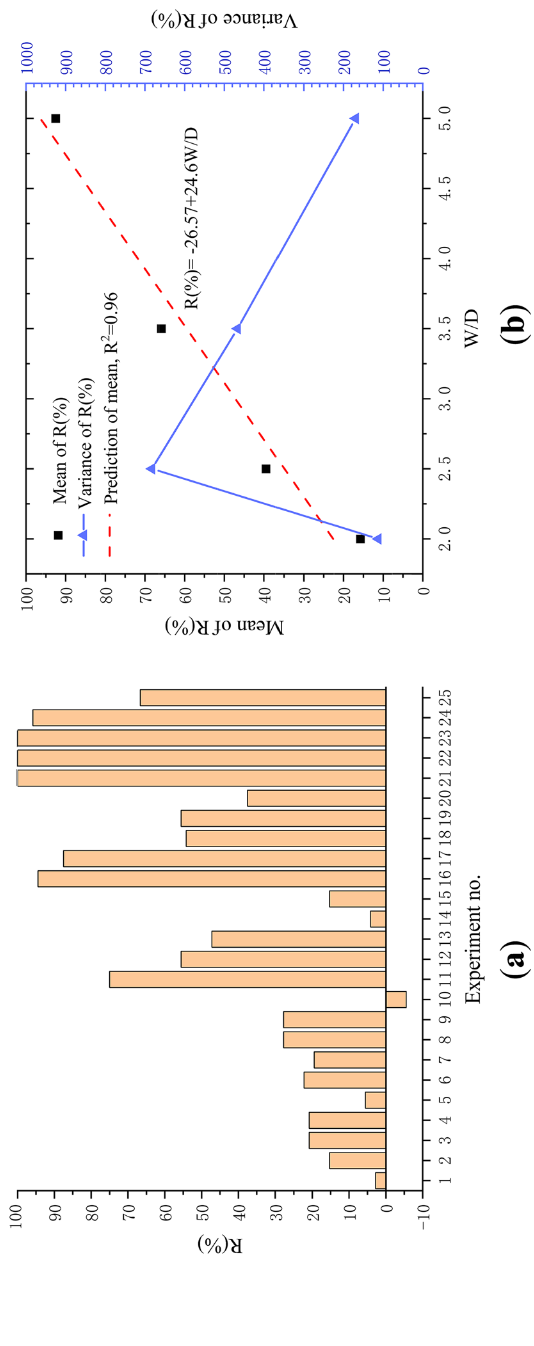

Fig. 9 **a** R (%) of the collar in experimental tests. **b** Means and variances of the R (%) of collar groups

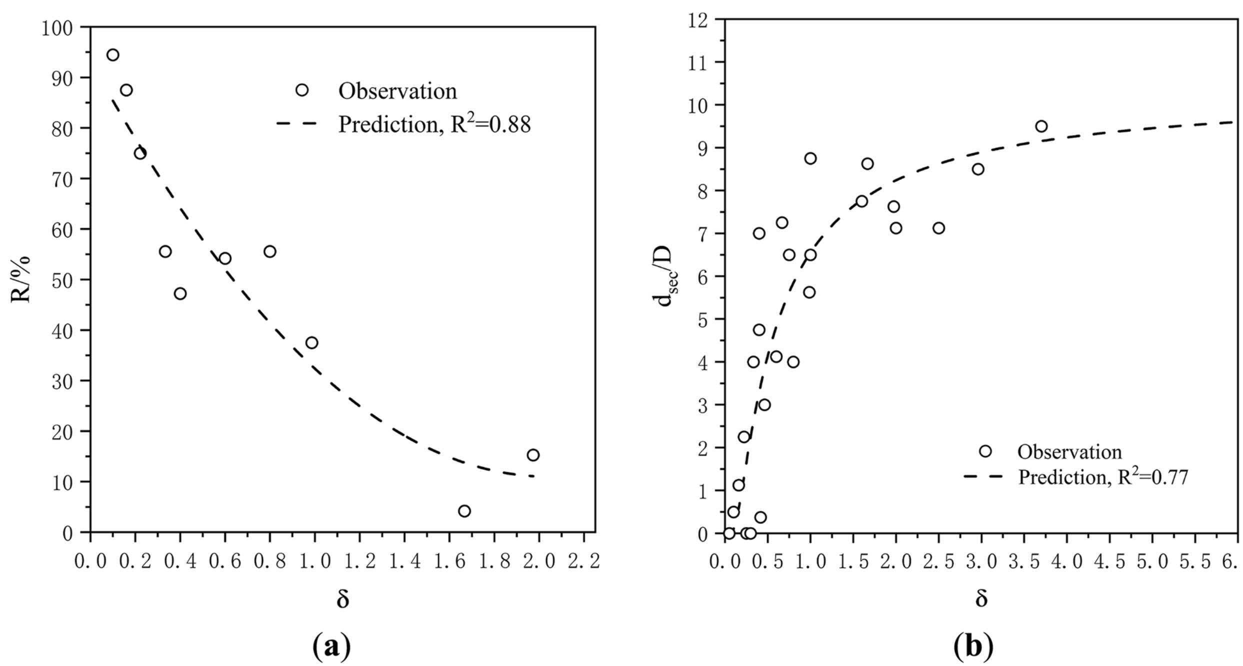

Fig. 10 Fitting results. **a** Prediction curve of the R (%). **b** Prediction curve of the maximum scour depth

$$d_{sec}/D = e^{a/\delta + b} \tag{12}$$

where a and b are the coefficients. The values of the coefficients can be obtained by least squares fitting, and finally, the equation to predict the maximum scour depth is as follows:

$$d_{sec}/D = e^{-0.424/\delta + 2.23} \tag{13}$$

Figure 10b shows the comparison between the observed and predicted values of the maximum scour depth around the pier. Obviously, there was an acceptable correlation between predicted values and the observed values.

Conclusions

In this study, a new type of bridge local scour countermeasure, i.e., horn-shaped collar, was investigated through model tests. Taguchi's method was used to design the test for reducing the number of experiments. Main effect analysis and ANOVA were introduced to determine the optimal design parameters of the horn-type collar. The main results of this study are concluded as follows:

1. The optimal bottom diameter, vertical height, and curvature shape index of the horn-shaped collar are 5*D*, 0.25*D*, and 4, respectively. In the case of optimal combination of parameters, the percent reduction of maximum scour depth around the bridge pier reaches 100%. Under the consideration of construction cost and availability, the design plan with a curvature shape index not less than 2 also satisfies the protection requirements. According to the results of ANOVA, the bottom diameter, vertical height, and curvature shape index have significant effects on the protective effect of the horn-shaped collar within the 90% confidence interval, and the bottom diameter of the collar has the largest contribution to the protective effect of the collar.
2. The bottom diameter and the curvature shape index of the horn-shaped collar are positively correlated with the scour reduction effect around the bridge pier, while the increase of the vertical height will weaken the protective effect of the horn-shaped collar.
3. Based on the experimental data, equations are developed to predict the average scour reduction rate of the horn-shaped collar with the variable bottom diameter and the maximum scouring depth around the bridge pier under the protection of the horn-shaped collar.

In the experiment, the influence of sand type and compactness on erosion are not considered. In addition, only one flow velocity is used, so there are certain limitations in the experiment. These limitations can be solved by subsequent model experiments and numerical simulation methods. Although there are some weaknesses in the experiment, the experimental results provide a reference for the design of three-dimensional collars such as horn-shaped collar. According to the experimental results, the horn-shaped collar has better anti-erosion potential, so it can be used in engineering practice.

Abbreviation

ANOVA Analysis of variance

Acknowledgements

The authors sincerely thank the anonymous reviewers for their valuable suggestions in improving the manuscript.

Authors' contributions

KL, designed the collar; YS, provided the procedure of the experiment; SL, contributed to interpretation of experimental results; all authors were involved in the writing and revision of the paper; and the authors read and approved the final manuscript.

Funding

This research was funded by the National Natural Science Foundation of China, grant number 51708043; Natural Science Basic Research Plan in Shaanxi Province of China, grant number 2019JQ-680; and Innovation and Entrepreneurship Training Programme for University Students, project number S202110710137.

Availability of data and materials

The datasets used and analyzed during the current study are available from the corresponding author on reasonable request.

Declarations

Competing interests

The authors declare that they have no competing interests.

Received: 16 August 2022 Accepted: 11 November 2022
Published online: 02 December 2022

References

1. Yi R, Zhou R (2015) Reason and risk of bridge collapse in recent 15 years. Transportation Technol Sci 05:61–64
2. Richardson E et al (1993) Evaluating scour at bridges. Federal Highway Administration, US Department of Transportation, Washington, DC
3. Ji B, Fu Z (2010) Analysis of Chinese bridge collapse accident causes in recent years. China Civ Eng J 43:495–498
4. Wang C, Yu X, Liang FY (2017) A review of bridge scour: mechanism, estimation, monitoring and countermeasures. Nat Hazards 87(3):1881–1906. https://doi.org/10.1007/s11069-017-2842-2
5. Paquier A et al (2018) Comparison between the circular and square collar in reduction of local scouring around bridge piers. E3S Web of Conf 40. https://doi.org/10.1051/e3sconf/20184003002
6. Wang C, Liang FY, Yu X (2017) Experimental and numerical investigations on the performance of sacrificial piles in reducing local scour around pile groups. Nat Hazards 85(3):1417–1435. https://doi.org/10.1007/s11069-016-2634-0
7. Cheng L et al (2012) Experimental research on protection of ring-wing pier against local scour. Adv Sci Technol Water Resour 32(3):14
8. Osroush M, Hosseini SA, Kamanbedast AA (2021) Countermeasures against local scouring around bridge abutments: combined system of collar and slot. Ijst-T Civ Eng 45(1):11–25. https://doi.org/10.1007/s40996-020-00443-4
9. Lauchlan CS, Melville BW (2001) Riprap protection at bridge piers. J Hydraul Eng 127(5):412–418
10. Chiew YM (1992) Scour protection at bridge piers. J Hydraul Eng 118(9):1260–1269
11. Valela C et al (2021) Hybrid modeling for design of a novel bridge pier collar for reducing scour. J Hydraul Eng 147(5). https://doi.org/10.1061/(Asce)Hy.1943-7900.0001875
12. Kumar V, Raju KGR, Vittal N (1999) Reduction of local scour around bridge piers using slots and collars. J Hydraul Eng 125(12):1302–1305
13. Wang SY et al (2019) Experimental investigation of local scour protection for cylindrical bridge piers using anti-scour collars. Water 11(7). https://doi.org/10.3390/w11071515
14. Dargahi B (1990) Controlling mechanism of local scouring. J Hydraul Eng 116(10):1197–1214
15. Jahangirzadeh A et al (2014) A cooperative expert based support vector regression (Co-ESVR) system to determine collar dimensions around bridge pier. Neurocomputing 140:172–184. https://doi.org/10.1016/j.neucom.2014.03.024
16. Raeisi N, Ghomeshi M (2021) A laboratory study of the effect of asymmetric-lattice collar shape and placement on scour depth and flow pattern around the bridge pier. Water Supply. https://doi.org/10.2166/ws.2021.239
17. Bestawy A et al (2020) Reduction of local scour around a bridge pier by using different shapes of pier slots and collars. Water Supply 20(3):1006–1015. https://doi.org/10.2166/ws.2020.022
18. Chen SC et al (2018) A hooked-collar for bridge piers protection: flow fields and scour. Water 10(9). https://doi.org/10.3390/w10091251
19. Valela C, Rennie CD, Nistor I (2022) Improved bridge pier collar for reducing scour. Int J Sediment Res 37(1):37–46. https://doi.org/10.1016/j.ijsrc.2021.04.004
20. Magar V et al (2014) Experimental and numerical investigation of the effect of different shapes of collars on the reduction of scour around a single bridge pier. PLoS ONE 9(6). https://doi.org/10.1371/journal.pone.0098592
21. Zhang R, Xie J, Chen W (2007) River dynamics. Wuhan University Press, Wuchang, Hubei, China
22. Melville BW, Coleman SE (2000) Bridge scour. Water Resources Publication, LLC, Highlands Ranch, CO, USA

23. Pandey M et al (2020) Reduction of time-dependent scour around piers using collars. Ocean Eng 213:15. https://doi.org/10.1016/j.oceaneng.2020.107692
24. Sheppard DM, Odeh M, Glasser T (2004) Large scale clear-water local pier scour experiments. J Hydraul Eng 130(10):957–963
25. Zhao M et al (2012) Experimental study of local scour around subsea caissons in steady currents. Coast Eng 60:30–40. https://doi.org/10.1016/j.coastaleng.2011.08.004
26. Roy RK (2010) A primer on the Taguchi method, 2nd edn. Society of Manufacturing Engineers, US

Publisher's Note

Springer Nature remains neutral with regard to jurisdictional claims in published maps and institutional affiliations.